ELSEVIER

Journal of Power Sources 64 (1997) 81–89

JOURNAL OF POWER SOURCES

Improvement of the formation efficiency of the tetrabasic lead sulfate for lead/acid batteries

L. Torcheux *, J.P. Vaurijoux, A. de Guibert

CEAC (EXIDE Europe), 5–7 allée des Pierres Mayettes, 92 636 Gennevilliers Cedex, France

Abstract

In the lead/acid battery manufacturing process, the formation of positive plates containing large needles of tetrabasic lead sulfate is very difficult to achieve. Today, the general solution to this problem consists in adopting a very long and expensive formation process with a large excess of Ah/kg. Even under these conditions, the extent of formation can be low. In this paper, we point out the difficulty to oxidize large 4BS needles because the crystal surface is covered by an insulating layer constituted of 0.2 μm interconnected $PbSO_4$ nodular grains. The thickness of this layer is small (nearly 1 μm) and is slightly but not sufficiently influenced by external conditions such as long soaking time, higher temperature, and optimization of current profile during formation. In this paper, we present a calculation model to forecast the formation efficiency of 4BS plates taking into account the crystal dimensions, the thickness of the sulfation layer and the complete composition of the positive active material before formation. Then, after comparison of this model with experimental values, the role of each parameter is examined and new conditions for a better formation are obtained. From these results, we suggest several solutions in order to improve the 4BS formation efficiency, and the corresponding results are given.

Keywords: Lead/acid batteries; Tetrabasic lead sulfate; Formation

1. Introduction

In the next few years, a challenge for lead/acid battery manufacturers should be a reduction of production costs while maintaining a good quality of the plates. Tetrabasic technology is useful to reach this goal but it will be necessary to improve the formation efficiency of such an active material.

The use of tetrabasic lead sulfate ($(PbO)_4 \cdot PbSO_4 = 4BS$) as an intermediary species instead of tribasic lead sulfate ($(PbO)_3 \cdot PbSO_4 \cdot H_2O = 3BS$) in the positive electrode is considered useful to avoid premature capacity loss (PCL) for lead/acid batteries [1,2].

Indeed, for flooded SLI batteries using Pb–Sb or Pb–Ca–Sn grid alloys, 4BS crystals have shown an ability to give high specific capacity after training (about 130 Ah/kg or 7.7 g/Ah) in the third consecutive low rate discharge. Therefore, this seems to be the safest way to avoid an eventual PCL for these batteries, and to ensure a better active material utilization allowing sensible reduction of the quantity of starting raw material for a higher battery quality.

The situation may be different for valve-regulated batteries with adsorptive glass material (AGM) or with gel technology. These batteries using Pb–Ca–Sn alloys and a low acid/matter ratio are more sensitive to charge acceptance problems after prolonged discharge owing to grid passivation [3–8]. The use of 4BS structures has also demonstrated a benefit for this problem. Nevertheless, there is a higher contribution of the cell design to PCL phenomena such as compression enhancement or various charge/discharge conditions, and this might overshadow the 4BS benefit for PCL.

Comparison between 4BS and 3BS crystallization shows crystals having an elongated prismatic form. However, the 4BS crystals are generally larger by a factor ten to twenty. There is a decrease in specific surface with the development of 4BS but this disadvantage is offset by the fact that the 4BS crystals are strongly interconnected to provide a stiff network. This porous matrix is therefore more robust than the 3BS counterpart which is composed of loose aggregates of smaller crystals. Moreover, 4BS structures provide more access for electrolyte to the centre of the matter and at the grid/matter interface. In that case, the use of 4BS active material with porous structure increases the acid concentration near the grid and then decreases the passivating α-PbO layer.

It is well known that the improvement of capacities is related to the 4BS content and mainly to the 4BS macrostructure [9,10] (the belief that 4BS promotes the α-PbO_2 polymorph which would give the positive plates a long cycle life is wrong). Indeed, the geometrical features of the 4BS

* Corresponding author.

PII S0378-7753(96)02506-2

structure are retained during the plate formation process, thus, the PbO_2 crystals remain better interconnected during cycling.

Unfortunately, the cured material consisted of large 4BS crystals is very difficult to oxidize. The core of the very big 4BS crystals remains generally unoxidized with the standard formation process (like 3BS formation). To overcome the problem of 4BS formation, the general solution consists in adopting a very long and expensive formation process with an Ah/kg excess. Even at these conditions, the extent of formation can be low. This point is a major issue in plants using 4BS technology, the time necessary for 4BS plate formation must be reduced to the 3BS material level.

2. Difficulties to form 4BS plates

It is now well established [1,10–16] that the 4BS oxidation mechanism proceeds from the 4BS crystal surface via 0.2 μm interconnected $PbSO_4$ nodular grains formed essentially during soaking and providing an insulating $PbSO_4$ layer. In spite of the small thickness (nearly 1 μm) of this layer, its compactness is a hindrance for ionic exchange and the sulfation of the crystal core is prevented leading to a low PbO_2 content. It results, after formation in poor first discharge capacities (first discharge capacity at C_{20} rate ($C/20$-1) is about 70–80 Ah/kg of PAM) and in low cell voltage on open circuit.

In order to improve 4BS formation, soaking conditions have been tested [17]. The influence of soaking time at different temperatures has been identified and the results are consistent with those observed by Lam et al. [15]. Indeed, the sulfation of 4BS seems to proceed via three different regimes: (i) at the beginning of soaking the crystal surface is fast converted into $PbSO_4$ nodules; (ii) the second is slower because the sulfation rate is small due to the insulating $PbSO_4$ layer formed by nodule agglomeration, and (iii) the third regime appears generally after long sulfation time (generally during the formation). In that case, some cracks are observed in the PbO_2 surface layer resulting from the differences of density of each layer (PbO_2/$PbSO_4$/4BS). Since these cracks give more access to the electrolyte, the sulfation of the crystal core is increased.

Moreover, it appears that 4BS oxidation is proportional to the sulfation layer thickness which itself is strongly influenced by temperature. Temperature increases the depth of sulfation and changes the granular $PbSO_4$ layer characteristics giving higher acid penetration toward the crystal core.

Another important observation is that the heat generation during the soaking time is proportional to the specific surface of active material. As a result the temperature increase during soaking is about twice lower for large 4BS than for 3BS material. Therefore, the acid should not be cooled before filling the batteries for 4BS material in order to obtain any benefit of the temperature effect during soaking. Furthermore, during formation it is necessary to include for 4BS a rest period allowing sulfation of crystal to restart without polarization.

The main conclusion of this study is that, in the industrial process soaking technology, small 3BS and large 4BS should not be treated in a similar way. The batteries with large 4BS (i.e. 100 μm) should wait 2 h after filling with non-cooled acid ($C/20$-1 is increased by 15% with 2 h soaking at $T = 55$ °C). On the other hand, for 3BS, the soaking time should not exceed 1 h and the batteries should be cooled as soon as possible before formation ($C/20$-1 is decreased by $\approx 5\%$ for soaking times > 1 h). According to Pavlov et al. [18], these results indicate that soaking should be introduced as a separate technological process.

Unfortunaly, these process adjustements are useful but do not improve sufficiently the formation of large 4BS crystals, and other solutions to this problem should be found.

Recently, very promising methods such as acid re-circulation or pulsed current formation [15] have been suggested for the purpose of solving this problem. For example, we have tested successfully pulsed formation with small discharge steps ($C/20$-1 is increased by 30%). Nevertheless, these techniques are too expensive and too difficult to be applied in factories.

Another method has been suggested to solve the 4BS formation problem [16] by reducing the size of the 4BS crystals without destroying the 4BS network in the PAM. The aim of this paper is to introduce this method and to define the optimum size for 4BS active material meeting easy formation and maintaining good perfomance in use.

3. Formation efficiency of 4BS plates

It is theoretically possible to relate the formation efficiency to the 4BS crystal size. For this purpose, we present hereafter a calculation model starting from X-ray diffraction (XRD) and scanning electron microscopy (SEM).

3.1. Description of the model

This model takes into account very simple considerations such as composition of the cured plate, 4BS crystal dimensions, the sulfation duration and the corresponding temperature. Other parameters such as porosity evolution, acid/matter ratio, total Ah received are not considered, but they will be discussed.

In order to forecast the first $C/20$ discharge capacity from the 4BS cured matter composition, we propose the following calculation considering that the 4BS matter consists of needles comparable with rectangular prisms (Fig. 1) and that the PbO_2 content produced from 4BS matter is directly related to the sulfated volume of each crystal. Therefore, with a simple calculation of the volume sulfated for one needle, it is possible to define a formation coefficient, $\bar{\tau}_i$, for the 4BS needle. For the total of 4BS crystals, this coefficient can be related to the mean dimensions of all needles

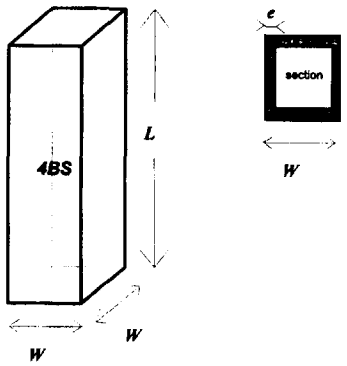

Fig. 1. 4BS needle.

$$\bar{\tau}=\sum\tau_i=\frac{(4\overline{LW}+2\bar{W}^2)e-(4\bar{L}+8\bar{W})e^2+8e^3}{\overline{LW^2}} \quad (1)$$

where L is the length, W the width of needles, and e the thickness of the sulfation layer. This thickness is related to the sulfation time and to the temperature. For example, with 20 h of sulfation ($d=1.24$ and $T=55$ °C) $e=1$ μm. This layer thickness has been measured by SEM on 4BS crystal cross sections after 20 h of formation.

In real conditions, cured plates contain not only 4BS crystals but also residual α- and β-PbO, free Pb, and in some cases other basic salts. It is well established that 3BS and residual PbO are easy to oxidize whereas it is more difficult to oxidize free Pb and 4BS. From this consideration it is possible to calculate the 'oxidizable' $Pb(II)_{ox}$ assuming that 3BS, α-, β-PbO are totaly oxidizable and that only the sulfated volume of 4BS crystal will be converted to lead dioxide. We will also consider that free lead (Pb(0)) is not oxidized to Pb(IV)

$$Pb(II)_{ox}=\frac{\%_{\alpha\text{-PbO}}}{M_{PbO}}+\frac{\%_{\beta\text{-PbO}}}{M_{PbO}}+4\frac{\%_{3BS}}{M_{3BS}}+5\bar{\tau}\frac{\%_{4BS}}{M_{4BS}} \quad (2)$$

$$Pb_{tot}=\frac{\%_{\alpha\text{-PbO}}}{M_{PbO}}+\frac{\%_{\beta\text{-PbO}}}{M_{PbO}}+4\frac{\%_{3BS}}{M_{3BS}}+5\frac{\%_{4BS}}{M_{4BS}}+\frac{\%_{Pb}}{M_{Pb}} \quad (3)$$

$$\chi=\frac{Pb(II)_{ox}}{Pb_{tot}} \quad (4)$$

where % represents the wt.% and M represents the molecular weight.

The ratio $Pb(II)_{ox}/Pb_{tot}$ gives that part of the lead which will be easily converted to PbO_2, this ratio represents the formation index contained between 0 and 1. Using these formulae, it is possible to calculate the formation index in relation to the composition, crystal dimension and sulfation conditions.

3.2. Results and comparison with the model

Automotive plates (Pb–Ca–Sn grids) with different compositions from different curing conditions have been used (active matter density about 4). Analyses of the cured samples were performed with an XRD INEL-CPS 120 spectrometer (PEAKS software [19]), porosities with a mercury porosimeter, SEM observations with JEOL-35CF microscope and specific surface measurements with the BET method.

Results are given in Table 1. Cured plates were formed at 440 Ah/kg of PAM during 20 h at constant current. The experimental setup is presented in Fig. 2 showing one positive plate contained between two negative plates. Purposely, we have not achieved complete 4BS formation for this experiment in order to simulate a short container formation. The

Table 1
Results of analysis and $C/20$ discharges of plates from different curing conditions [a]

Ref.	α-PbO (wt.%)	β-PbO (wt.%)	Pb (wt.%)	3BS (wt.%)	4BS (wt.%)	Porosity (cm^3/g)	Mpr (μm)	SBET (cm^2/g)	4BS size		C/20-1	C/20-2	C/20-3	C/20-4
									L (μm)	W (μm)	(Ah/kg of PAM)			
A	46	0.7	4	0	49	0.131	2.94	0.52	80	18	73	109	116	128
B	52	0.5	2.8	0	45	0.132	2.29	0.60	80	20	76	105	117	125
C	42	0.7	1.5	0	46	0.140	1.94	0.77	60	12	77	108	111	119
D	50	0.5	0.8	0.6	49	0.133	1.25	0.75	60	12	78	103	115	124
E	50	1.8	1	1.7	45	0.125	0.82	0.68	50	12	81	109	114	121
F	37	1.4	1.2	1.2	59	0.133	1.45	0.86	50	9	85	110	111	120
G	55	0.9	5.1	2.3	37	0.121	1.11	0.90	50	10	88	104	109	117
H	55	0.7	2.9	6.2	35	0.127	0.59	0.97	50	10	97	109	112	119
I	60	0.6	1.4	6.9	31	0.122	0.57	0.91	55	12	98	107	107	111
J	58	0.8	1.5	7.9	32	0.123	0.52	0.99	50	10	108	109	111	120
K	62	0	3.1	8.3	27	0.131	0.51	1.08	50	10	109	111	113	113
L	60	5.1	2.4	18.4	14	0.115	0.35	1.15	50	9	112	105	107	106
M	63	3.6	3.7	13.8	16	0.123	0.48	1.15	50	9	125	107	97	96
N	61	10	0.2	28	0	0.112	0.35	1.08	nd	nd	125	124	124	123
O	59	10	0.1	26	1.4	0.128	0.37	1.12	nd	nd	125	122	122	120

[a] nd: not detectable.

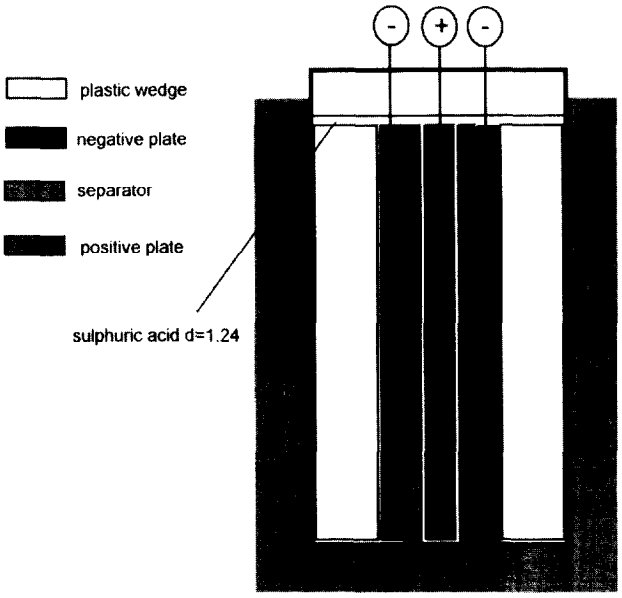

Fig. 2. Experimental cell.

initial acid density was 1.24, acid/matter ratio was about 3 cm^3/g, and temperature was maintained at 55 °C. After formation, the plates were discharged at a $C/20$ rate ($T=25$ °C until the final voltage 1.70 V) and were recharged with one theoretical capacity (120 Ah/kg) at the $C/20$ rate. Then, the plates were cycled (discharged at $C/20$ rate and recharged with 115% of discharged Ah). The acid/matter ratio in this cell involves a large excess of acid and that is obviously not representative of cycling conditions in batteries, this influence on our study will be discussed.

The results of the four first discharge capacities are presented in Table 1. It can be observed that the first discharge capacity depends on the curing conditions, as expected. The correlation between the 4BS content, mean pore radius (Mpr) and first discharge capacities are given in Figs. 3 and 4. It is shown that the formation is influenced by the 4BS content and by the 4BS size (Mpr is mainly related to the crystal size). When the 4BS content and the Mpr increased

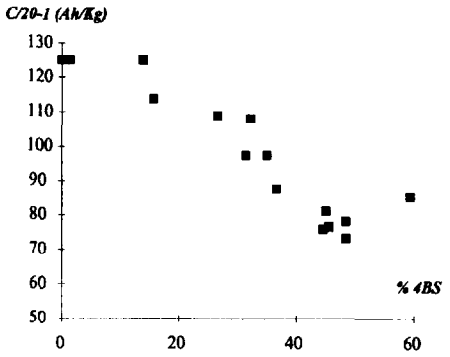

Fig. 3. $C/20$-1 evolution vs. 4BS content.

the formation efficiency is decreased. Fig. 4 shows that experimental points fit with an exponential decay law (Eq. (5))

$$C/20-1_{(\mathrm{Ah/kg})} = 62.1 + 32.9 \exp -\frac{(\mathrm{Mpr}-0.4)}{0.27} + 21.6 \exp -\frac{(\mathrm{Mpr}-0.4)}{4.3} \quad (5)$$

This empirical law relates the first discharge capacity to the Mpr of the cured plate. It is observed that the fit is poor for intermediate values of Mpr.

In order to compare results of the model with those experimentally obtained we have converted formation index in capacities (125 Ah/kg of PAM for $\chi=1$). The precision of the model has been estimated by using the accuracy on intervening parameters:

1. composition by XRD (Peaks software) $\rightarrow \pm 5\%$;
2. measurement of the crystal sizes by SEM $\rightarrow \bar{L} \pm 5$ μm, $\bar{W} \pm 2$ μm;
3. measurement of the sulfation layer thickness $\rightarrow e \pm 0.1$ μm.

The result of this calculation gives a standard deviation of ± 0.04 on the modelized formation index ($\pm 6\%$ if $\chi=0.75$). Moreover, we will consider that the experimental $C/20$-1 is given with standard deviation of $\pm 2\%$. Using these consid-

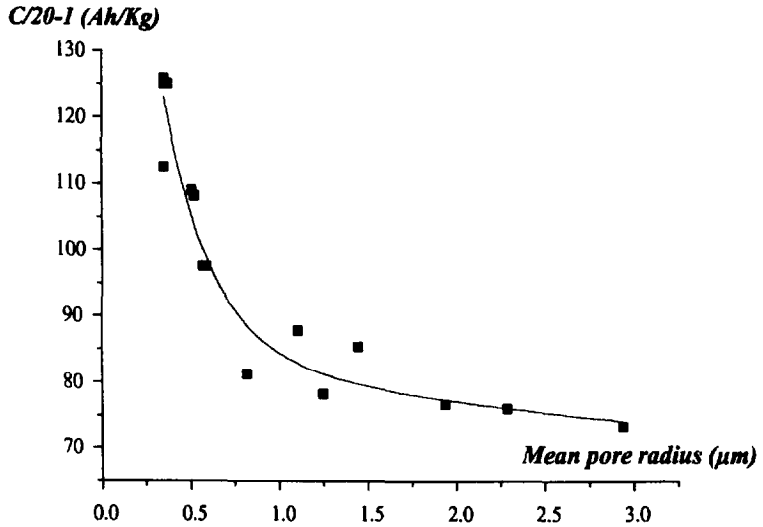

Fig. 4. $C/20$-1 evolution vs. mean pore radius.

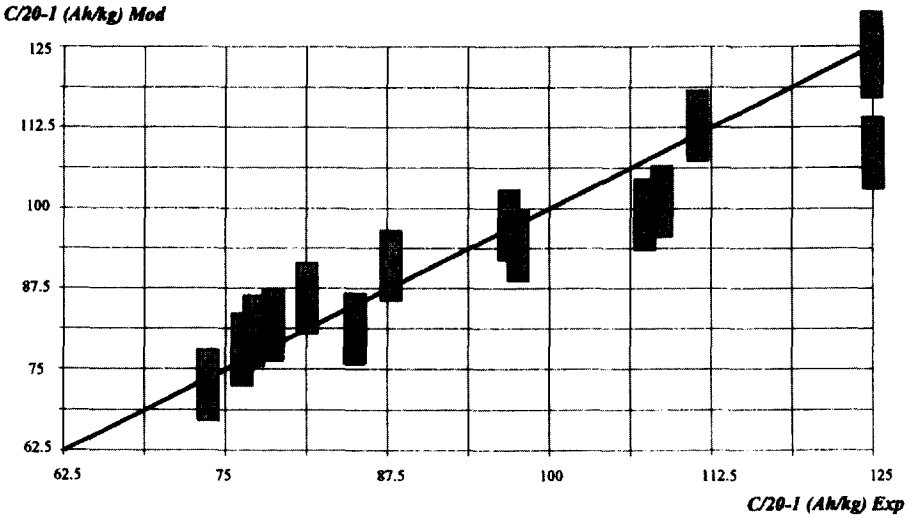

Fig. 5. Correlation graph between experimental and calculated $C/20$-1.

erations it is possible to obtain a graph (Fig. 5) showing the correlation between experimental and calculated first discharge capacities. The line $C/20\text{-}1_{mod} = C/20\text{-}1_{exp}$ repr. nts 100% agreement.

A good agreement is observed for most of the plates (taking into account the above mentioned margin error) except for plates containing about 10% of 3BS (J, K, M) which are experimentally better formed than expected.

The calculation does not take into account the parameters such as porosity evolution and acid/matter ratio.

Fig. 6 shows that the total porosity of 4BS plates is only slightly affected by sulfation, in contrast to the 3BS material. Therefore, we may consider that this parameter does not induce a significant error in the calculation for this kind of plates because all the material is in contact with the same high acid density.

Concerning the acid/matter ratio the situation is more complicated because the characteristics of the insulating sulfation layer on 4BS crystals depends on the SO_4^{2-} activity near the positive plates. For example, a low ratio may result either in a smaller thickness of the insulating sulfation layer or may change the structure of this layer (increase the size of $PbSO_4$ nodules) favouring deep sulfation by increasing the microporosity. In these latter two cases, the effect on the formation efficiency is not the same. On the other hand, a large acid/matter ratio may develop a more insulating $PbSO_4$ layer on the 4BS crystal surface (nucleation is more pronounced) and could impede a deep sulfation in the crystal core. This parameter should be more studied, but our protocol with a large acid/matter ratio (3 cm^3/g) is probably not advantaged in comparison with the real case.

To conclude, although this model is simple and do not use all the contributing parameters it seems to be well adapted and sufficient to forecast the behaviour of the 4BS PAM formation with good accuracy.

3.3. Influence of the parameters and discussion

The influence of several parameters on the formation index has been studied in order to define new 4BS active material characteristics for better formation using our calculation.

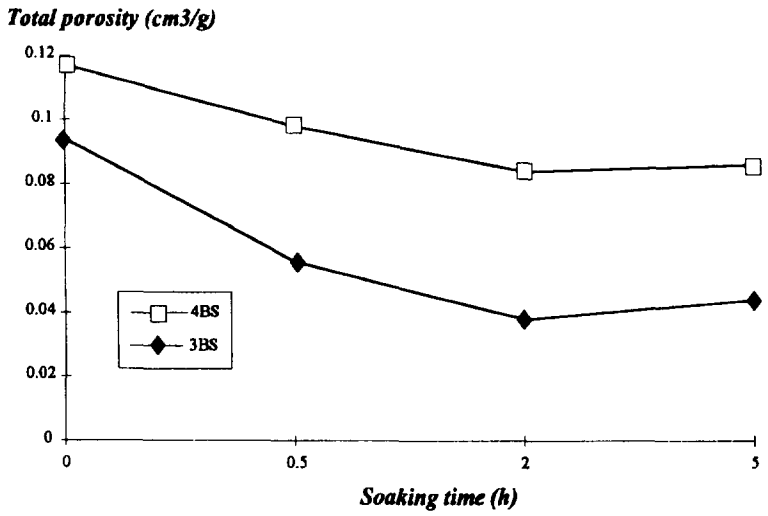

Fig. 6. Evolution of PAM total porosity with soaking time in excess of sulfuric acid, $d = 1.24$.

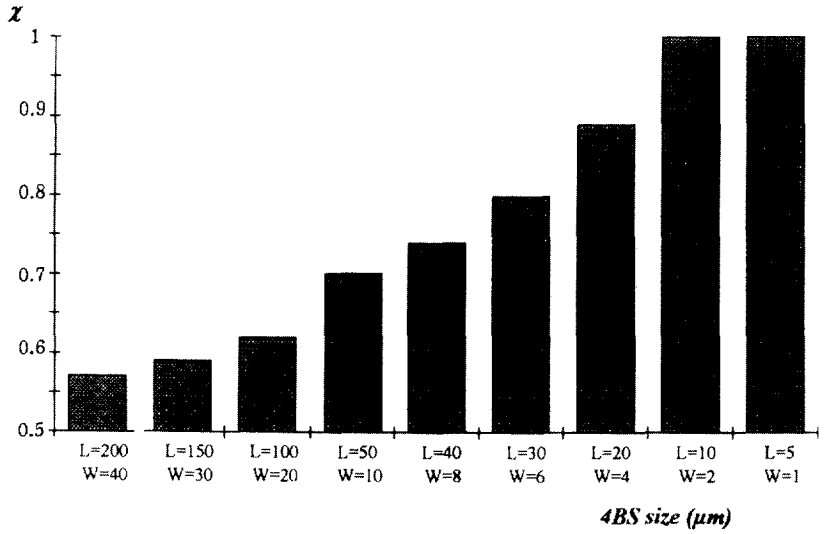

Fig. 7. Influence of 4BS crystal dimensions on the formation index.

Fig. 7 shows the influence of the 4BS crystal size on formation index. It has been assumed in the calculation that the dimension of 4BS exhibits a ratio $L/W = 5$. Plates considered were constituted by 50% of residual PbO and by 50% of 4BS. The sulfation layer thickness is 1 μm. These results show that the formation is very dependent on the 4BS size and could be largely improved by reducing its dimensions.

Length and width of 4BS crystals have been decomposed in order to understand their respective role (Fig. 8(a) and (b)). When the needle width is constant (10 μm), it is shown that the increase in 4BS crystal length does not affect the formation index. On the other hand, if the length is constant (50 μm), the formation index is strongly affected by the increase in width. It is interesting to observe that long 4BS crystals with relative small width should be easy to form.

The calculated formation index evolution in relation to the ratio PbO/4BS for plates consisting of 4BS crystals with three different widths (5, 10, 20 μm) is given Fig. 9. It shows that formation difficulties are related to the increase of the 4BS content. This effect was expected (Table 1) for the same crystal characteristics: the higher the 4BS content, the higher the difficulty to form the plate. However, it is well shown by calculation that this effect is enhanced for large crystal sections. Furthermore, the influence of the sulfation layer thickness reported in Fig. 10, regarding three different 4BS crystal widths (5, 10, 20 μm), shows well the benefit of a long soaking duration which is more remarkable for smaller 4BS crystal widths.

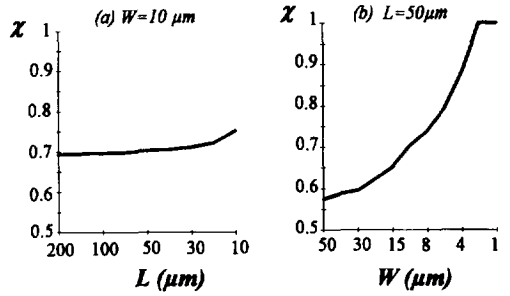

Fig. 8. Influence of (a) length and (b) width of 4BS crystal on the formation index.

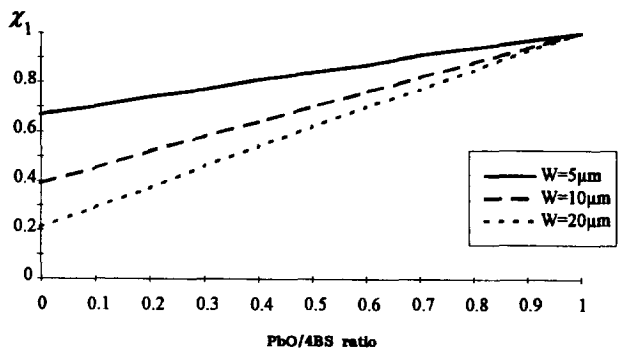

Fig. 9. Influence of the chemical composition on the formation index for three different 4BS widths.

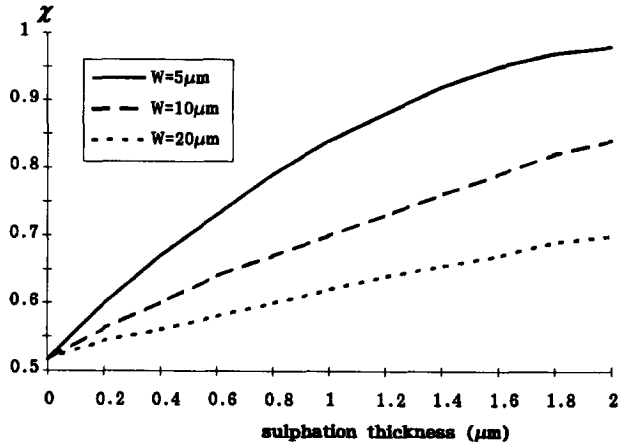

Fig. 10. Influence of the thickness of the sulfation layer on the formation index for three different 4BS widths.

4. Proposals to improve the formation efficiency of 4BS plates

Since 4BS crystals with large dimensions are very difficult to form, the solution to this problem could be the manufacturing of plates with only 3BS or a mixture of 4BS/3BS which shows a better formation behaviour. Nevertheless, the problem should not only be treated in terms of formation efficiency. The *C*/20-2, *C*/20-3, *C*/20-4 discharges (Table 1) show that PAM with the biggest crystals gives higher and more stable capacities after training. This result is due to the large crystals presenting a strong skeleton and a better material utilization owing to a better PbO_2 crystal interconnection. This condition is generally not respected with 3BS or 3BS/4BS mixtures leading to a better formation but resulting in lower capacities after training. These structures show weaker networks and generally more PCL depending on the cell design and on the acid content and access. However, in some cases it has been observed that 3BS/4BS mixtures are convenient to limit the capacity decay during the first cycles.

Smaller width between 4BS needles combined with a good management of soaking conditions should be a very convenient way to improve formation. 4BS plates with the following characteristics should present a very good behaviour in formation:

composition → α-PbO ≈ 50%, 4BS ≈ 50%, Pb ≈ 1%, and

crystal size → $L \approx 30$–100 μm, $W \approx 5$ μm.

The soaking time should be kept between 1 and 2 h without cooling device, and a rest period be included during formation. For this type of matter the calculation gives a formation index close to 0.9, thus, the first discharge capacities should be comparable with those obtained with 3BS matter. Capacities and cycling results with this material should be good because the length of such 4BS crystals remains sufficiently high to prevent a fast destruction of the matter network and to ensure a good crystal interconnection.

In this way, new conditions for 4BS crystallization should be tested. In most of the cases, the proposed solutions result from the change of parameters controlling nucleation/growth equilibria and/or the use of additives.

4.1. First results of new crystallization conditions for 4BS

The influence of several parameters during the paste process on the 4BS crystal size have been already mentioned by Ozgun et al. [20]. They showed that when a low acid-to-oxide ratio is used the 4BS crystal size decreases.

Another method without paste modification could be to change the 4BS crystallization process after pasting. In this way, we have tested the influence of different conditions during the high temperature period. Unfortunately, by reducing the temperature to 80 °C (Fig. 11) instead of 100 °C (Fig. 12) resulted not only in a small decrease of the 4BS crystal size but also of that in the 3BS/4BS mixtures. These mixtures were easier to form but the PAM network is intermittent.

During the high temperature period, the preponderant parameter for 4BS crystal size seems to be the level and the loss rate of the moisture contained in the plates. This can be easily observed with plates presenting two different thicknesses but with the same initial moisture. After the same high temperature period one may observe that the thinner plates present coarser 4BS crystals (Fig. 13) than the thicker plates which lose moisture at a smaller rate (Fig. 14).

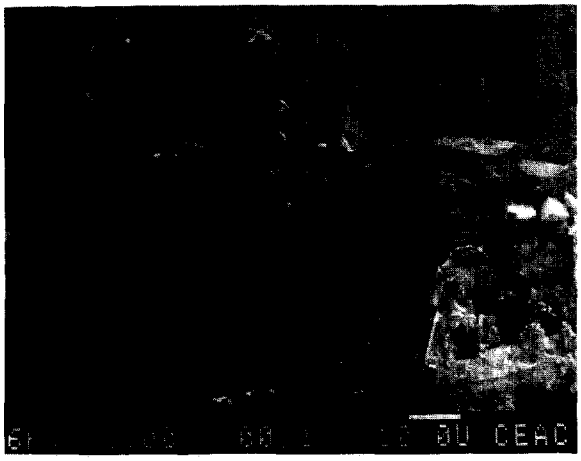

Fig. 11. PAM cured at 80 °C during 2 h.

Fig. 12. PAM cured at 100 °C during 2 h.

Fig. 13. PAM cured at 100 °C during 2 h, thin plates.

Fig. 14. PAM cured at 100 °C during 2 h, thick plates.

Fig. 15. PAM cured at 100 °C during 2 h, with high initial moisture and with low rate of water loss.

To explain this behaviour we can assume that for the same high temperature (100 °C), intermediary species are dissolved in different amounts of water films formed around the crystals seeds. Humidity loss during this period plays an important role by increasing the activities of these species and influences the diffusion of dissolved species towards crystal seeds leading to higher crystal dimensions.

In this case, larger 4BS crystals are obtained with high initial plate humidities combined with high rate of water loss. On the other hand, the same initial moisture with small rates of water loss gives smaller 4BS crystals. This has been successfully tested and it resulted in small 4BS crystals ($L = 30$ μm, $W = 5$ μm, Fig. 15). Batteries assembled with this kind of plate have demonstrated very stable high $C/20$ capacities without major problems in formation.

This method seems to meet our goals but it is nevertheless difficult to control in factories because it requires a very fine control of humidity in the flash dryer and in the curing chambers. Moreover, heterogeneities may occur because the loss of humidity is often not the same for the centre plates as for the edge plates.

Another method consists in considering, in a better way, the parameters which have an influence on the 4BS nucleation. This can be observed by using pure presulfated oxide in the paste. This results in very small 4BS crystals ($L = 10$ μm, $W = 2$ μm, Fig. 16). In this process the nucleation of 4BS crystals is largely favoured against the growth of needles. However, although this material has met easy formation it has not revealed high improvement in PCL (crystals remain small). The solution to this problem could be the use of small quantities of presulfated oxide as the additive in the oxide to find a method to increase the nucleation in the standard process. In particulary, the role of the oxide should be studied thoroughly and subsequent investigations at the mixing step should be carried out. This work will be presented in a future paper.

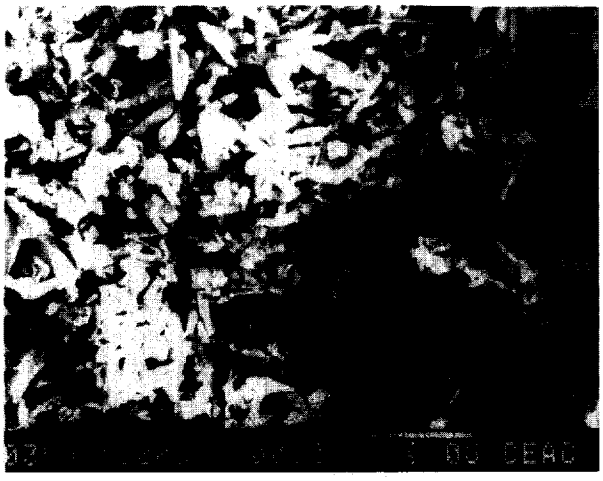

Fig. 16. PAM obtained with pure presulfated oxide and cured at 60 °C.

5. Conclusions

A reduction of manufacturing costs and maintaining the quality of batteries could be obtained by the use of the 4BS technology if formation problems can be solved. In this paper, a method has been proposed mainly based on the reduction of the 4BS crystal size (especially the needle section) giving significant improvement. It has been shown that this size can be controlled with simple process adjustments. This study suggests also that it could be very interesting to produce long 4BS crystals presenting a small section. This material should give PAM with a very high interconnection degree combined with high porosity and high specific surface. This could be another step allowing sensible reduction of starting raw material without affecting battery quality.

Acknowledgements

The authors would like to express their thanks to J.M. Lebourgeois, O. Paccaud and M. Bassini for their help in the industrial tests and plate preparation.

References

[1] D. Pavlov and N. Kapkov, *J. Electrochem. Soc., 137* (1990) 21.
[2] R.V. Biagetti and M.C. Weeks, *Bell Syst. Tech. J., 49* (1970) 1305.
[3] D. Pavlov, B. Monakhov, M. Maya and N. Penazzi, *J. Electrochem. Soc., 136* (1989) 27.
[4] J. Garche, *J. Power Sources, 30* (1990) 47–54.
[5] H. Döring, J. Garche, H. Dierz and K. Weisener, *J. Power Sources, 30* (1990) 41–45.
[6] K. Takahashi, H. Yasuda, N. Takami, S. Horie and Y. Suzui, *UNESCO Expert Workshop: Theory and Practice of the Lead/Acid System, Gaussig, Germany, 2–5 Apr. 1991.*
[7] A.F. Hollenkamp, *J. Power Sources, 36* (1991) 567–585.
[8] K. Takahashi, N. Hoshihara, H. Yasuda, T. Ishii and H. Jimbo, *J. Power Sources, 30* (1990) 23–31.
[9] B. Culpin, *J. Power Sources, 25* (1989) 305–311.
[10] L.T. Lam, A.M. Vecchio-Sadus, H. Ozgun and D.A.J. Rand, *J. Power Sources, 38* (1992) 87–102.
[11] J. Burbank, *J. Electrochem. Soc., 113* (1966) 10.
[12] D. Pavlov, G. Papazov and V. Iliev, *J. Electrochem. Soc., 119* (1972) 8.
[13] D. Pavlov and E. Bashtavelova, *J. Power Sources, 31* (1990) 243–254.
[14] K.R. Bullock, B.K. Mahato and W.J. Wruck, *J. Electrochem. Soc., 138* (1991) 35.
[15] L.T. Lam, H. Hozgun, L.M.D. Cranswick and D.A.J. Rand, *J. Power Sources, 42* (1993) 55.
[16] L.T. Lam and D.A.J. Rand, *Batteries Int.*, (Oct.) (1992) 52.
[17] S. Grugeon-Deweale, A. Delahaye-Vidal, J.B. Leriche, J.M. Tarascon, L. Torcheux, J.P. Vaurijoux, F. Henn and A. de Guibert, *J. Power Sources*, submitted for publication.
[18] D. Pavlov, S. Ruevski and T. Rogachev, *J. Power Sources, 46* (1993) 337–348.
[19] R.J. Hill, A.M. Foxworthy and R.J. White, *J. Power Sources, 32* (1990) 3.
[20] H. Ozgun, L.T. Lam, D.A.J. Rand and S.K. Bhargava, *J. Power Sources, 32* (1990) 3.